Int. J. Heat Mass Transfer. Vol. 36, No. 5, pp. 1287–1294, 1993
Printed in Great Britain

0017-9310/93 $6.00 + 0.00
Pergamon Press Ltd

Variable viscosity effects on the vortex instability of free convection boundary layer flow over a horizontal surface in a porous medium

JIIN-YUH JANG† and JIN-SHENG LEU
Department of Mechanical Engineering, National Cheng-Kung University, Tainan, Taiwan 70101, R.O.C.

(*Received* 12 *May* 1992)

Abstract—The role of temperature-dependent viscosity is studied in the flow and vortex instability of a heated horizontal free convection boundary layer flow in a saturated porous medium. For an isothermal surface, similarity solutions are found to exist for viscosity variation expressed as a general function of temperature. For exponential variation of viscosity with temperature, the numerical results for Nusselt number, critical Rayleigh number and associated wave number at the onset of vortex instability are presented over a wide range of wall to ambient viscosity ratio parameters. It is found that the variable viscosity effect enhances the heat transfer rate and destabilizes the flow for liquid heating, while the opposite trend is true for gas heating.

1. INTRODUCTION

WHEN NATURAL convection heat transfer takes place under conditions where there are large temperature differences within the fluid, it is necessary (for accuracy) to consider the effects of variable fluid properties. Analysis of natural convection boundary layer flow with variable viscosity in a viscous fluid has been performed rather extensively (see, for example, ref. [1], and the references cited therein). The results showed that variable viscosity has a significant effect on the thermal and momentum transport predictions. However, the analogous problem of natural convection boundary layer flow in a saturated porous medium has received rather little attention. Earlier studies have considered mostly the variable viscosity effects on the onset of convection in a horizontal porous layer bounded by two parallel plates heated from below.

Kassoy and Zebib [2] examined the variable viscosity effects on the onset of convection in a water-saturated porous medium. The temperature difference between the top and bottom is as large as 250°C. The effects of an eight-fold variation in kinematic viscosity are included. The critical Rayleigh number is found to be substantially reduced from the classical value of $4\pi^2$ for the Benard problem of porous media. Straus and Schubert [3] and Horne and O'Sullivan [4] also considered the onset of convection of water as a non-Boussinesq fluid with viscosity and thermal expansivity dependence. The reported critical Rayleigh number is reduced by as much as a factor of 31 below the classical value of $4\pi^2$.

Gary *et al.* [5] investigated the effects of significant viscosity variation on convective heat transport in water-saturated porous media in a rectangular cavity. It was found that the flow and temperature fields became unstable at even moderate values of the Rayleigh number and exhibited a fluctuating convective state analogous to that observed for the constant viscosity case. Blythe and Simpkins [6] applied an integral method to examine the natural convection in a two-dimensional cavity filled with fluid-saturated porous media for the case in which the viscosity is temperature-dependent. The variable viscosity effect on natural convection in an internally heat-generating porous medium in a short, vertical circular cylinder was studied by Dona and Stewart [7]. Recently, Ramrez and Saez [8] studied the forced convection boundary layer flow in a saturated porous medium containing a fluid with temperature-dependent viscosity. Lai and Kulacki [9] investigated the effect of variable viscosity on mixed convection boundary layer flow around a vertical surface in a saturated porous medium. In refs. [8, 9], the linear variation of viscosity is assumed. Therefore, they cannot satisfy most of the engineering applications, except for very small wall and ambient temperature differences.

The flow and vortex modes of instability in natural convection boundary layer flow over a horizontal or an inclined heated plate in a saturated porous medium with constant viscosity have been the subject of studies of Cheng and Chang [10], Hsu *et al.* [11], and Hsu and Cheng [12]. Jang and Chang [13] re-examined the same problem for an inclined plate, where both the streamwise and normal components of the buoyancy forcer are retained in the momentum equations. Therefore, ref. [13] provides new vortex instability results for small angles of inclination from the hori-

† To whom correspondence should be addressed.

NOMENCLATURE

a	dimensional spanwise wave number
d	temperature difference, $T_w - T_\infty$
f	similarity stream function profile
F	dimensionless disturbance stream function amplitude, $\tilde{\psi}/[ia(Ra_x)^{1/3}]$
g	gravitational acceleration
k	dimensionless wave number, $ax/(Ra_x)^{1/3}$
K	permeability
Nu_x	local Nusselt number
Nu_L	average Nusselt number for plate length L
p'	perturbation pressure
p	pressure
Ra_x	local Rayleigh number, $\rho_\infty g\beta K(T_w - T_\infty)x/\mu_\infty\alpha$
S	a general function for viscosity variation with temperature
T	temperature
T'	perturbation temperature
$\tilde{T}$	disturbance temperature amplitude
$\tilde{u}$	x direction disturbance velocity amplitude
u, v, w	volume averaged velocity in the x, y, z directions
u', v', w'	disturbance velocity in the x, y, z directions
x, y, z	axial, normal and spanwise coordinates.

Greek symbols

α	effective thermal diffusivity
β	coefficient of thermal expansion
η	similarity variable, $y(Ra_x)^{1/3}/x$
θ	dimensionless temperature, $(T - T_\infty)/(T_w - T_\infty)$
Θ	dimensionless disturbance temperature amplitude, $\tilde{T}/(T_w - T_\infty)$
μ	absolute dynamic viscosity
μ'	disturbance dynamic viscosity
ν	kinematic viscosity
ρ	density
υ^*	wall to ambient viscosity ratio, $\upsilon^* = \upsilon_w/\upsilon_\infty$
ψ	stream function
ψ'	disturbance stream function
$\tilde{\psi}$	disturbance stream function amplitude.

Subscripts

w	condition at the wall
∞	condition at the free stream.

Superscript

*	critical condition.

zontal ($\phi \leqslant 30°$) and more accurate results for large angles of inclination ($\phi > 30°$) than the previous study [12]. Later, Jang and Chang [14] studied the vortex instability of horizontal natural convection in a porous medium resulting from combined heat and mass buoyancy effects. The effects of a density extremum on the vortex instability of an inclined buoyant layer in porous media saturated with cold water were examined by Jang and Chang [15, 16].

All of these works are based on the Darcy formulation. However, at a higher Rayleigh number or in a high porosity medium, there is a departure from Darcy's law and the inertia, convective, thermal dispersion and boundary effects not included in the Darcy model may become significant. Recently, Chang and Jang [17, 18] were the first authors to study the non-Darcy effect on the vortex instability of a horizontal natural convection boundary layer flow in a saturated porous medium. However, the variable viscosity effect on the vortex instability of natural convection boundary layer flow over a horizontal plate does not seem to have been investigated. This motivated the present investigation.

The present study examines in detail the effects of temperature-dependent viscosity on the flow and vortex instability of natural convection boundary layer flow adjacent to a heated horizontal surface embedded in a saturated porous medium. The variation of viscosity with temperature is represented by an exponential function, which is more accurate than a linear function for large temperature differences. In the base flow, similarity solutions are obtained for the case of an isothermal boundary condition. The analysis of the disturbance flow is based on linear stability theory. The resulting eigenvalue problem is solved using a variable step size sixth-order Runge–Kutta integration scheme in conjunction with the Gram–Schmidt orthogonalization procedure [19] to maintain the linear independence of the eigenfunctions.

2. MATHEMATICAL ANALYSIS

Before proceeding to the instability problem, consideration is given first to the basic natural convection flow along a heated horizontal surface, since the computation of instability criteria requires a knowledge of the velocity and temperature profiles for the base flow and the solution has not been investigated before.

2.1. *The base flow*

The physical model and the coordinate system are shown in Fig. 1, where x represents the distance along the plate from its leading edge and y the distance normal to the surface. If we assume that: (1) local

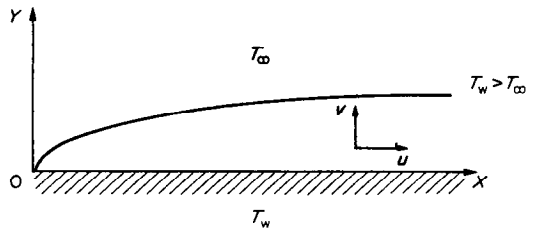

FIG. 1. The physical model and coordinate system.

thermal equilibrium exists between the fluid and solid phases, (2) the physical properties are considered to be constant, except for the density ρ and absolute viscosity μ, (3) the Boussinesq and boundary layer approximations are employed, then the governing equations based on Darcy's law are given by:

$$\frac{\partial u}{\partial x}+\frac{\partial v}{\partial y}=0 \tag{1}$$

$$u=-\frac{K}{\mu}\frac{\partial p}{\partial x} \tag{2}$$

$$v=-\frac{K}{\mu}\left\{\frac{\partial p}{\partial y}+\rho_\infty g[1-\beta(T-T_\infty)]\right\} \tag{3}$$

$$u\frac{\partial T}{\partial x}+v\frac{\partial T}{\partial y}=\alpha\frac{\partial^2 T}{\partial y^2}. \tag{4}$$

The absolute viscosity μ is assumed to vary with temperature according to a general function form $\mu=\mu_\infty S(T)$, where μ_∞ is the absolute viscosity at the ambient temperature and therefore $S(T_\infty)=1$.

Similarity analysis proceeds by employing a stream function such that $u=\partial\Psi/\partial y$ and $v=-\partial\Psi/\partial x$ and by defining

$$\eta=yb(x) \qquad \Psi(x)=c(x)f(\eta)$$

$$\theta=\frac{T-T_\infty}{T_w-T_\infty} \quad d(x)=T_w(x)-T_\infty. \tag{5}$$

Substituting equation (5) into equations (2)–(4), the momentum and energy equations become

$$S(T)f''=-dS'(T)f'\theta'-\frac{\rho_\infty g\beta K}{\mu_\infty}\left[\frac{d_x}{cb^2}\theta+\frac{ydb_x}{cb^2}\theta'\right] \tag{6}$$

$$\theta''=\frac{cd_x}{\alpha db}f'\theta-\frac{c_x}{\alpha b}f\theta \tag{7}$$

where the primes (for functions f and θ) and the subscript x indicate derivatives with respect to η and x, respectively.

The functions b, c, d and S must be such that x and T disappear from equations (6) and (7). These require that

$$d(x)=T_w-T_\infty=\text{constant}$$

$$b(x)=(Ra_x)^{1/3}/x, \quad c(x)=\alpha(Ra_x)^{1/3} \tag{8}$$

where $Ra_x=\rho_\infty g\beta K(T_w-T_\infty)x/\mu_\infty\alpha$ is the local Rayleigh number, in which the dynamic viscosity is evaluated at T_∞.

Substituting equation (8) into equations (6) and (7), results in

$$S(T)f''=-dS'(T)f'\theta'+\tfrac{2}{3}\eta\theta' \tag{9}$$

$$\theta''=-\tfrac{1}{3}f\theta'. \tag{10}$$

It can be seen that similarity exists for the case of an isothermal surface (i.e. $d=$ constant) if $S(T)$ is a function of η only. This is true if $S(T)$ is a function of θ. The ambient temperature corresponds to $\theta=0$. Thus $\mu=\mu_\infty S(\theta)$ and $S(0)=1$. A wide variety of functional forms of $S(T)$ satisfy this requirement, for example: algebraic expressions, power series, exponential forms, etc.

It is necessary, before proceeding, to choose a particular viscosity–temperature relation. The one adopted was a compromise between simplicity and satisfactory agreement with experimental data. An exponential relation, $\mu=B\exp(AT)$, seems most appropriate to fulfil these conditions (see Table 1), where A and B are constants adopted from the least square fitting for a particular fluid. In this case, it can be shown that

$$S(T)=\exp[A(T-T_\infty)]=(v^*)^\theta \tag{11}$$

where $v^*=v_w/v_\infty=\exp[A(T_w-T_\infty)]$ is the wall to ambient viscosity ratio parameter. Substituting the exponential form of $S(T)$ into equation (9), one may have

$$f''=-(\ln v^*)f'\theta'+\tfrac{2}{3}\eta v^{*(-\theta)}\theta' \tag{12}$$

$$\theta''=-\tfrac{1}{3}f\theta'. \tag{13}$$

For the case of $v^*=1$ the equations reduce to the two-dimensional base flow equations for constant viscosity evaluated at the ambient temperature [10]. The transformed boundary conditions are

$$f(0)=f'(\infty)=\theta(0)-1=\theta(\infty)=0. \tag{14}$$

The local and average Nusselt numbers are as follows:

$$\frac{Nu_x}{Ra_x^{1/3}}=-[\theta'(0)], \quad \frac{Nu_L}{Ra_L^{1/3}}=-3\theta'(0). \tag{15}$$

2.2. *The disturbance flow*

In the usual manner for linear stability analysis, the velocities, pressure, temperature and viscosity are assumed to be the sum of mean and fluctuating components, here denoted as barred and primed quantities, respectively,

$$u(x,y,z,t)=\bar{u}(x,y)+u'(x,y,z,t)$$

$$v(x,y,z,t)=\bar{v}(x,y)+v'(x,y,z,t)$$

$$w(x,y,z,t)=w'(x,y,z,t)$$

$$p(x,y,z,t)=\bar{p}(x,y)+p'(x,y,z,t)$$

$$T(x,y,z,t)=\bar{T}(x,y)+T'(x,y,z,t)$$

$$\mu(T)=\bar{\mu}(\bar{T})+\mu'. \tag{16}$$

Table 1. The values of A and B for different fluids; the viscosity unit is centipoise

Fluid	Air	Water	Spindle oil [20]	Silicone DC F-60 [20]	Mobiltherm 600 oil [20]
Temperature range	25–275°C	20–100°C	25–75°C	25–75°C	25–75°C
Pr_∞ (25°C)	0.72	7	178	667	2148
A	0.001515	−0.01577	−0.02928	−0.02223	−0.05136
B	0.01883	1.286	24.29	106.02	437.88
% error compared to ref. [20]	1.18	3.23	3.63	1.95	5.6

After substituting equation (16) into the governing equations for the three-dimensional convective flow in a porous medium, subtracting the parts satisfied by the base flow quantities, and linearizing the disturbance quantities, we arrive at the following equations for the disturbances:

$$\frac{\partial u'}{\partial x}+\frac{\partial v'}{\partial y}+\frac{\partial w'}{\partial z}=0 \tag{17}$$

$$\bar{\mu}u'+\bar{u}\mu'=-K\frac{\partial p'}{\partial x} \tag{18}$$

$$\bar{\mu}v'+\bar{v}\mu'=-K\left(\frac{\partial p'}{\partial y}-\rho_\infty g\beta T'\right) \tag{19}$$

$$w'=-\frac{K}{\bar{\mu}}\frac{\partial p'}{\partial z} \tag{20}$$

$$\bar{u}\frac{\partial T'}{\partial x}+\bar{v}\frac{\partial T'}{\partial y}+u'\frac{\partial \bar{T}}{\partial x}+v'\frac{\partial \bar{T}}{\partial y}=\alpha\left(\frac{\partial^2 T'}{\partial x^2}+\frac{\partial^2 T'}{\partial y^2}+\frac{\partial^2 T'}{\partial z^2}\right). \tag{21}$$

Following the method of order-of-magnitude analysis described in detail by Hsu *et al.* [11], the terms $\partial u'/\partial x$, $\partial^2 T'/\partial x^2$ in equations (17) and (21) can be neglected. The omission of $\partial u'/\partial x$ in equation (17) implies the existence of a disturbance stream function ψ' such that

$$v'=-\frac{\partial \psi'}{\partial z},\quad w'=\frac{\partial \psi'}{\partial y}. \tag{22}$$

We assume that the three-dimensional disturbances are of the form

$$(\psi',u',T')=[\tilde{\psi}(x,y),\tilde{u}(x,y),\tilde{T}(x,y)]\exp(iaz+q(x)) \tag{23}$$

where a is the spanwise periodic wave number, and

$$q(x)=\int \alpha_i(x)\,dx$$

with $\alpha_i(x)$ denoting the spatial growth factor. For the lowest order approximation, $q(x)=\alpha_i x$. Setting $\alpha_i=0$ for neutral stability yields

$$ia\tilde{u}+ia\bar{u}(\ln \nu^*)\frac{\tilde{T}}{T_w-T_\infty}-(\ln \nu^*)\frac{\partial \tilde{\psi}}{\partial y}\frac{\partial \theta}{\partial x}=\frac{\partial^2 \tilde{\psi}}{\partial x\,\partial y} \tag{24}$$

$$(\nu^*)^\theta\frac{\partial^2 \tilde{\psi}}{\partial y^2}-(\nu^*)^\theta a^2\tilde{\psi}-ia\bar{v}(\nu^*)^\theta(\ln \nu^*)\frac{\tilde{T}}{T_w-T_\infty}+(\nu^*)^\theta(\ln \nu^*)\frac{\partial \tilde{\psi}}{\partial y}\frac{\partial \theta}{\partial y}=-\frac{iaK\rho_\infty g\beta}{\mu_\infty}\tilde{T} \tag{25}$$

$$\alpha\left(\frac{\partial^2 \tilde{T}}{\partial y^2}-a^2\tilde{T}\right)=\bar{u}\frac{\partial \tilde{T}}{\partial x}+\bar{v}\frac{\partial \tilde{T}}{\partial y}+\tilde{u}(T_w-T_\infty)\frac{\partial \theta}{\partial x}-ia\tilde{\psi}(T_w-T_\infty)\frac{\partial \theta}{\partial y}. \tag{26}$$

Letting

$$k=\frac{ax}{Ra_x^{1/3}},\quad F(\eta)=\frac{\tilde{\psi}}{i\alpha Ra_x^{1/3}},\quad \Theta(\eta)=\frac{\tilde{T}}{T_w-T_\infty} \tag{27}$$

we obtain the following system of equations

$$(\nu^*)^\theta[F''+(\ln \nu^*)\theta' F'-k^2F]=-kRa_x^{1/3}[1-(\nu^*)^\theta(\ln \nu^*)Ra_x^{-2/3}(\tfrac{2}{3}\eta f'-\tfrac{1}{3}f)]\Theta \tag{28}$$

$$\Theta''+\tfrac{1}{3}f\Theta'-[k^2+\tfrac{2}{3}(\ln \nu^*)\eta\theta' f']\Theta=\frac{2\eta\theta'}{9kRa_x^{1/3}}\{2\eta F''+[1+2(\ln \nu^*)\eta\theta']F'\}+kRa_x^{1/3}\theta' F \tag{29}$$

with the boundary conditions given by

$$F(0)=\Theta(0)=F(\infty)=\Theta(\infty)=0 \tag{30}$$

where the primes indicate the derivative with respect to η. Equation (30) arises from the fact that the disturbances vanish at the wall and in the free stream in a porous medium. Equations (28)–(30) constitute a fourth-order system of linear ordinary differential

equations for the disturbance amplitude distributions $F(\eta)$ and $\Theta(\eta)$. For fixed v^*, solutions of $F(\eta)$ and $\Theta(\eta)$ are eigenfunctions for the eigenvalues Ra_x and k. For the case of $v^* = 1$, the equations reduce to the conventional disturbance equations for the constant viscosity assumption [11] with viscosity evaluated at the ambient temperature.

3. NUMERICAL METHOD OF SOLUTION

In the stability calculations, the disturbance equations are solved by separately integrating two linearly independent integrals. The full solution may be written as the sum of two linearly independent solutions

$$F(\eta) = F_1(\eta) + EF_2(\eta)$$
$$\Theta(\eta) = \Theta_1(\eta) + E\Theta_2(\eta). \tag{31}$$

Two independent integrals (F_i, Θ_i), with $i = 1, 2$, may be chosen so that their asymptotic solutions are

$$F_1 = \exp(-k\eta_\infty), \qquad \Theta_1 = 0$$
$$F_2 = \frac{A_1}{A_2^2 - k^2}\exp(-A_2\eta_\infty), \quad \Theta_2 = \exp(-A_2\eta_\infty) \tag{32}$$

where

$$A_1 = -[1 + \tfrac{1}{3}(\ln v^*)Ra_x^{-2/3}f_\infty]kRa_x^{1/3}$$
$$A_2 = \frac{f_\infty}{6} + \left[\left(\frac{f_\infty}{6}\right)^2 + k^2\right]^{1/2}. \tag{33}$$

A sixth-order variable step size Runge–Kutta integration routine is used here to solve first the base flow system, equations (12) and (13), and the results are stored for a fixed step size, $\Delta\eta = 0.02$, which is small enough to predict accurate linear interpolation between mesh points. Equations (28) and (29) with boundary conditions (30) are then solved as follows. For specified v^* and k, Ra_x is guessed. Using equations (32) as starting values, the two integrals are integrated separately from the outer edge of the boundary layer to the wall using a sixth-order Runge–Kutta variable step size integrating routine incorporated with the Gram–Schmidt orthogonalization procedure [19] to maintain the linear independence of the eigenfunctions. The required input of the base flow to the disturbance equations is calculated, as necessary, by linear interpolation of the stored base flow. From the values of the integrals at the wall, E is determined using the boundary condition $F(0) = 0$. The second boundary condition, $\Theta(0) = 0$, is satisfied only for an appropriate value of the eigenvalue Ra_x. A Taylor series expansion of the second condition provides a correction scheme for the initial guess of Ra_x. Iterations continue until the second boundary condition is sufficiently close to zero (typically $< 10^{-6}$).

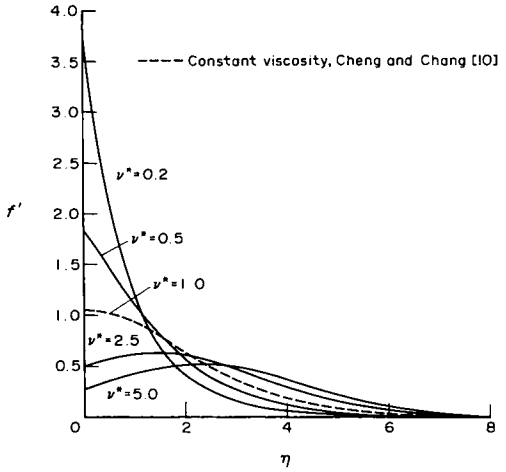

FIG. 2. Velocity profile across the boundary layer for various values of v^*.

4. RESULTS AND DISCUSSION

Numerical results for the tangential velocity, temperature profiles, Nusselt number, neutral stability curves, the critical Rayleigh number and wave number at the onset of vortex instability are presented for a range of wall to ambient viscosity ratio parameter v^* from 0.1 to 10. As the temperature is increased, the liquid viscosity decreases, while the gas viscosity increases. Therefore, for a heated wall, values of $v^* < 1$ correspond to the case of liquid heating, and values of $v^* > 1$ correspond to the case of gas heating.

Figures 2 and 3 show the tangential velocity and temperature profiles across the boundary layers for selected values of v^* (0.2, 0.5, 1, 2.5 and 5). The dashed lines denote the traditional constant viscosity results ($v^* = 1$) with the viscosity evaluated at the ambient temperature; the present results are in good agreement with those of Cheng and Chang [10]. Because the viscosity in the liquid (or gas) decreases (or increases) with increasing temperature, a larger (or smaller) vel-

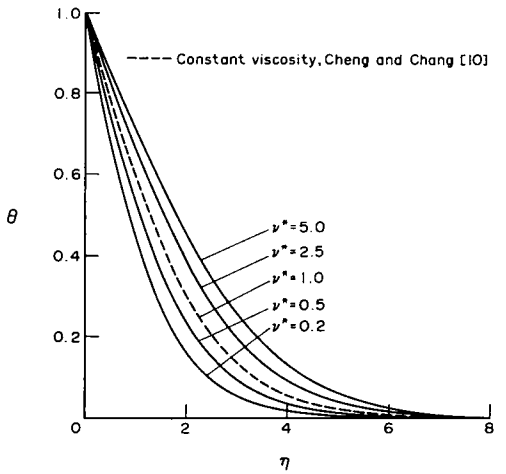

FIG. 3. Temperature profile across the boundary layer for various values of v^*.

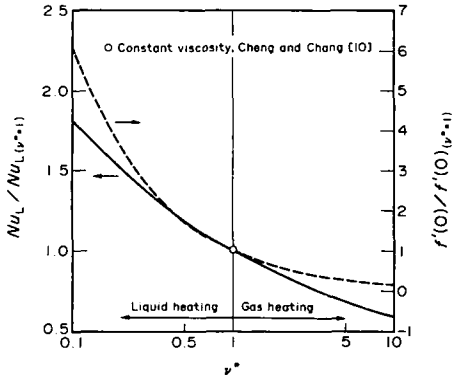

FIG. 4. The variation of Nusselt number and slip velocity with various values of v^*.

ocity near the wall is expected for a heated wall. This agrees with the theoretical results shown in Fig. 2. It is also found that the effect of temperature-dependent viscosity on the velocity profiles is more pronounced than the effect on temperature profiles. Non-unity values of v^* alter both the position and magnitude of the maximum velocity relative to that for the constant viscosity results ($v^* = 1$), as well as altering the temperature gradient at the wall.

Figure 4 shows the alteration of Nusselt number and slip velocity with v^*. The values are normalized by their respective values for the case of constant viscosity ($v^* = 1$). It is seen that the constant viscosity results underestimate the Nusselt number for liquid heating and overestimate it for gas heating. For example, for a 10-fold variation in kinematic viscosity, the constant viscosity result based on the ambient temperature [10] would be underestimated by 75% for liquid heating ($v^* = 0.1$) and overestimated by 40% for gas heating ($v^* = 10$). It is interesting to note that for a heated wall, Darcy's slip velocity may be reduced to zero due to the increase of the gas viscosity if the wall to ambient viscosity ratio is sufficiently large ($v^* \approx 10$).

Figure 5 shows the neutral stability curve, in terms

Table 2. Critical Rayleigh numbers and the associated wave number for various values of v^*

v^*	Ra_x^*	k^*
0.1	23.272	1.3894
0.2	25.791	1.0496
0.5	29.586	0.8021
1.0	33.028	0.6853
2.5	38.275	0.5769
5.0	42.176	0.5106
10.0	44.735	0.4517

of the Rayleigh number Ra_x and the dimensionless wave number k, for selected values of v^* (0.2, 0.5, 1, 2.5, 5 and 10). It is observed that for liquid heating ($v^* < 1$), the neutral stability curves shift to lower Rayleigh number and higher wave number, indicating a destabilization of the flow, while for gas heating ($v^* > 1$), the opposite trend is true. When the realistic variable viscosity effects are included, the reason for liquid heating (or gas heating) being more (or less) susceptible to instability than the traditional constant viscosity [11] result is due to reduction (or increase) in the dissipative effects of viscosity.

The critical Rayleigh number Ra_x^* and associated wave number k^*, which mark the onset of longitudinal vortices, can be found from the minima of the neutral stability curves. These critical values are listed in Table 2 for selected values of v^* and are also plotted in Fig. 6. For $v^* = 1$, the critical Rayleigh number and wave number are computed to be 33.028 and 0.6853, respectively, as compared to 33.47 and 0.692 reported in Hsu *et al.* [11] appropriate for the constant viscosity case. It is seen that, for $v^* = 0.1$ (liquid heating), the critical Rayleigh number is reduced by about 30% relative to the constant viscosity result ($v^* = 1$), while for $v^* = 10$ (gas heating), the critical Rayleigh number is increased by about 36%. The numerical results also indicate that as the viscosity parameter v^* increases, the critical Rayleigh number increases and the associated wave number decreases.

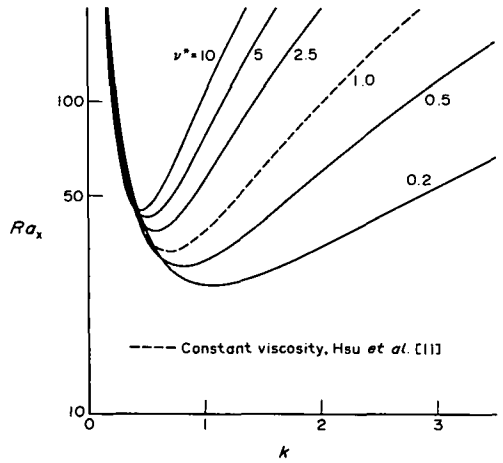

FIG. 5. Neutral stability curves for various values of v^*.

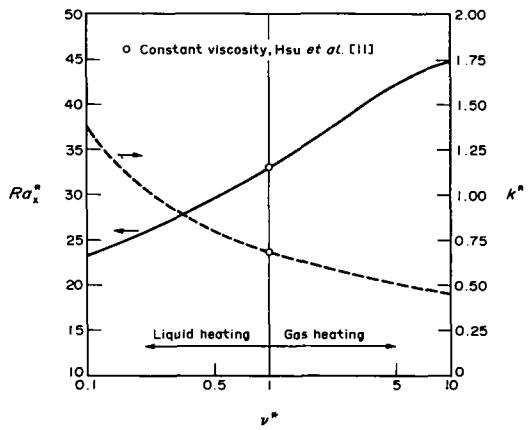

FIG. 6. Critical Rayleigh number and associated wave number for various values of v^*.

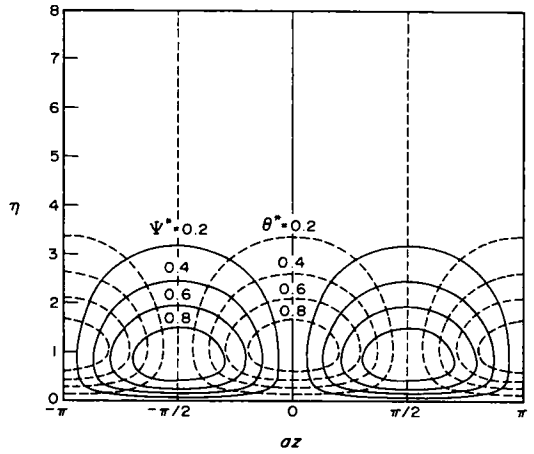

FIG. 7. The streamlines (solid lines) and isotherms (dashed lines) of the secondary flow at the onset of instability for $v^* = 0.2$ (liquid heating).

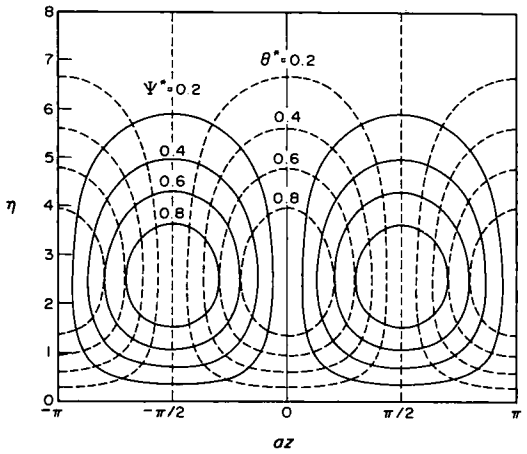

FIG. 9. The streamlines (solid lines) and isotherms (dashed lines) of the secondary flow at the onset of instability for $v^* = 2.5$ (gas heating).

Figures 7–9 show the streamlines and isotherms for the secondary flow at the onset of instability for $v^* = 0.2$ (liquid heating), 1 (constant viscosity) and 2.5 (gas heating), respectively. The results show a relatively high density of steamlines near the heated wall for liquid heating when compared to the constant viscosity case and a relatively low density of streamlines for gas heating. Therefore, the major effect of viscosity variation is to concentrate the convection in the lower part of the boundary layer, where reduced viscosity (liquid heating) tends to destabilize the flow, while increased viscosity (gas heating) tends to stabilize the flow.

5. CONCLUSIONS

A viscosity parameter, $v^* = v_w/v_\infty$, has been successfully employed in a stability analysis to include the exponential temperature dependence of viscosity in the natural convection boundary layer adjacent to an isothermal horizontal plate embedded in a saturated porous medium. The present results predict that variable viscosity has a significant effect on temperature and velocity profiles as well as the Nusselt numbers and critical Rayleigh numbers. It is shown that, for liquid heating, the variable viscosity effect enhances the heat transfer rate and destabilizes the flow; for gas heating, the opposite is true. As the viscosity parameter v^* increases, the critical Rayleigh number increases and the associated wave number decreases.

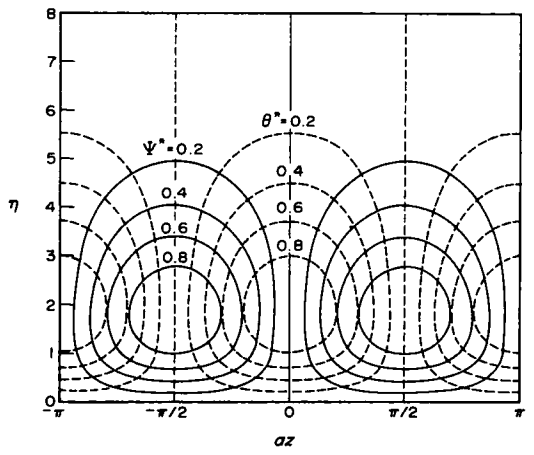

FIG. 8. The streamlines (solid lines) and isotherms (dashed lines) of the secondary flow at the onset of instability for $v^* = 1.0$ (constant viscosity).

REFERENCES

1. V. P. Carey and J. C. Mollendorf, Variable viscosity effects in several natural convection flows, *Int. J. Heat Mass Transfer* **23**, 95–109 (1980).
2. D. R. Kassoy and A. Zebib, Variable viscosity effects on the onset of convection in a porous media, *Phys. Fluids* **18**, 1649–1651 (1975).
3. J. M. Straus and G. Schubert, Thermal convection of water in a porous medium: effects of temperature- and pressure-dependent thermodynamic and transport properties, *J. Geophys. Res.* **82**, 325–333 (1977).
4. R. N. Horne and M. J. O'Sullivan, Convection in a porous medium heated from below: the effect of temperature-dependent viscosity and thermal expansion coefficient, *J. Heat Transfer* **100**, 448–452 (1978).
5. J. Gary, D. R. Kassoy, H. Tadjeran and A. Zebib, The effects of significant viscosity variation on convective heat transport in water-saturated porous media, *J. Fluid Mech.* **117**, 233–249 (1982).
6. P. A. Blythe and P. G. Simpkins, Convection in a porous layer for a temperature dependent viscosity, *Int. J. Heat Mass Transfer* **24**, 497–506 (1981).
7. C. L. G. Dona and W. E. Stewart, Variable property effects on convection in a heat generating porous medium, *J. Heat Transfer* **111**, 1100–1102 (1989).
8. N. E. Ramrez and A. E. Saez, The effect of variable viscosity on boundary-layer heat transfer in a porous medium, *Int. Commun. Heat Mass Transfer* **17**, 477–488 (1990).
9. F. C. Lai and F. A. Kulacki, The effect of variable viscosity on convective heat transfer along a vertical surface in a saturated porous medium, *Int. J. Heat Mass Transfer* **33**, 1028–1031 (1990).

10. P. Cheng and I.-D. Chang, Buoyancy-induced flows in a saturated porous medium adjacent to impermeable horizontal surfaces, *Int. J. Heat Mass Transfer* **19,** 1267–1272 (1976).
11. C. T. Hsu, P. Cheng and G. M. Homsy, Instability of free convection flow over a horizontal impermeable surface in a porous medium, *Int. J. Heat Mass Transfer* **21,** 1221–1228 (1978).
12. C. T. Hsu and P. Cheng, Vortex instability in buoyancy-induced flow over inclined heated surfaces in porous media, *J. Heat Transfer* **101,** 660–665 (1979).
13. J. Y. Jang and W. J. Chang, Vortex instability of buoyancy-induced inclined boundary layer flow in a saturated porous medium, *Int. J. Heat Mass Transfer* **31,** 759–767 (1988).
14. J. Y. Jang and W. J. Chang, The flow and vortex instability of horizontal natural convection in a porous medium resulting from combined heat and mass buoyancy effects, *Int. J. Heat Mass Transfer* **31,** 769–777 (1988).
15. J. Y. Jang and W. J. Chang, Vortex instability of inclined buoyant layer in porous media saturated with cold water, *Int. Commun. Heat Mass Transfer* **14,** 405–416 (1987).
16. J. Y. Jang and W. J. Chang, Maximum density effects on vortex instability of horizontal and inclined bouyancy induced flows in porous media, *J. Heat Transfer* **111,** 572–574 (1989).
17. W. J. Chang and J. Y. Jang, Inertia effects on vortex instability of a horizontal natural flow in a saturated porous medium, *Int. J. Heat Mass Transfer* **32,** 541–550 (1989).
18. W. J. Chang and J. Y. Jang, Non-Darcian effects on vortex instability of a horizontal natural convection flow in a porous medium, *Int. J. Heat Mass Transfer* **32,** 529–539 (1989).
19. A. R. Wazzan, T. T. Okamura and H. M. O. Smith, Stability of laminar boundary layers at separation, *Phys. Fluids* **10,** 2540–2545 (1967).
20. P. L. Geiringer, *Handbook of Heat Transfer Medium.* Reinhold, New York (1962).